ChemComm

Accepted Manuscript

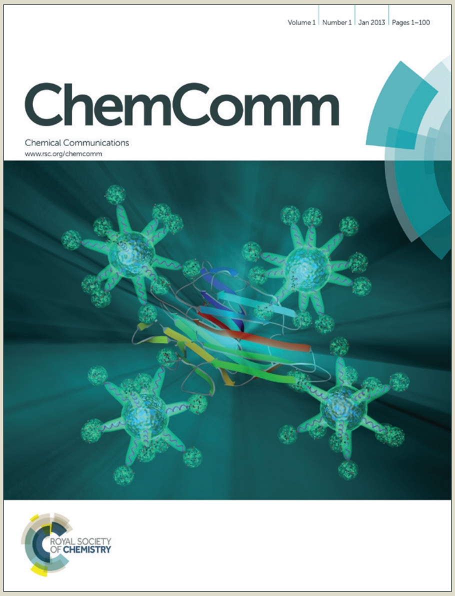

ChemComm RSCPublishing

COMMUNICATION

Highly-effective gating of single-molecule junctions: an electrochemical approach

Cite this: DOI: 10.1039/x0xx00000x

Received 00th January 2012,
Accepted 00th January 2012

DOI: 10.1039/x0xx00000x

www.rsc.org/

Masoud Baghernejad,[a#] David Zsolt Manrique,[b#] Chen Li,[a] Thomas Pope,[b] Ulmas Zhumaev,[a] Ilya Pobelov,[a] Pavel Moreno-García,[a] Veerabhadrarao Kaliginedi,[a] Cancan Huang,[a] Wenjing Hong,[a]* Colin Lambert,[b*] and Thomas Wandlowski[a]

We report an electrochemical gating approach with ~100% efficiency to tune the conductance of single-molecule 4,4'-bipyridine junctions using scanning-tunnelling-microscopy break junction technique. Density functional theory calculation suggests that electrochemical gating aligns molecular frontier orbitals relative to the electrode Fermi-level, switching the molecule from an off resonance state to "partial" resonance.

The idea of using individual molecules as building blocks of electronic devices was first proposed by Aviram and Ranter.[1] Various experimental approaches have been employed to create single-molecule junctions between two metal electrodes.[2] To realize the full potential of single-molecule electronic devices it is desirable to incorporate a third (gate) electrode, which can tune the energy levels of the molecule.[3] Understanding and exploring efficient gating mechanisms is important for the development of future low-energy-consumption single-molecule electronic devices. Reported gating efficiency is still limited to less than 40%,[4] and therefore optimization of gating efficiency remains a major challenge.

The concept of "electrochemical gating" has been employed in the gating of single-molecule junctions to tune the molecular energy levels relative to the Fermi energy E_F of the source and drain electrodes. A correlation exists between relative electrochemical potential with reference to standard hydrogen electrode (SHE) and absolute energy level E(abs) that $E(abs)/V = E(SHE)/V + 4.44$ for aqueous system,[5] which suggests that the electrochemical gating provides 100% gating efficiency from applied electrochemical potential to energy level shift of the electrodes in principle. This concept has been previously employed in electrochemical active molecular systems including viologens,[3c, 3d] oligoaniline,[3b] ferrocene,[6] transition metal complexes,[7] redox-active proteins,[8] and quinone and anthraquinone.[9] On the other hand, this approach is also promising for electrochemical inactive molecules for which redox processes can be excluded.[4a] In this respect, 44BPy is a good candidate molecule for electrochemical control, because of its well defined binding geometry.[2a, 10] In recent works, the energy level alignment of 44BPy was probed via thermopower measurement[11] and electrochemical behavior of 44BPy was studied over a broad potential range without structure transition.[12]

In this communication, we present charge transport studies of an electrochemically-inactive 44BPy molecule, contacted to source-drain electrodes under electrochemical potential control using an STM-based break junction (STMBJ, Scheme 1).[13] Remarkably we found that the applied electrochemical potential allows the tuning of molecular levels with respect to the Fermi energy E_F of the electrodes with almost 100% efficiency without any molecular structure change of 44BPy. Density functional theory (DFT) calculations were employed to obtain the origin of these three conductance states and to provide quantitative understanding of our experimental investigation.

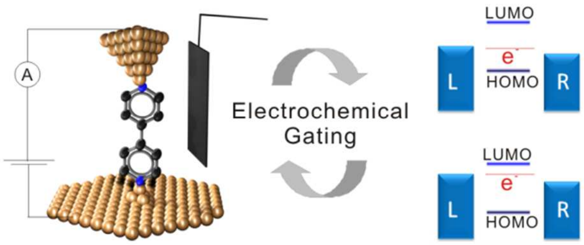

Scheme 1. Electrochemical gate effect of applied potential.

The STM break junction measurement of 44BPy was first carried out in $KClO_4$ electrolyte containing 0.5 mM 44BPy on Au(111) surface at applied potential 120 mV vs. Hg/Hg_2SO_4 (MSE). As shown in Figure 1A, after a sharp decrease in conductance related to breaking of the gold-gold contact, the molecule bridges the electrode gap causing plateaus at conductances $G \leq 10^{-3}G_0$, denoted H, M, and L, which are attributed to the formation of (single) molecular junctions. In figures 1B and 1C, three conductances (H, M, and L) with high-density data clouds are observed in the conductance range $1.0\times10^{-4.5}$ $G_0 \leq G \leq 1.0\times 10^{-2.5}$ G_0, centered on $10^{-2.9}$, $10^{-3.3}$, and $10^{-3.9}$ G_0. These are in good agreement with previous studies[10, 14] except for the first time, the H conductance feature was observed in aqueous electrolytes under potential control, because of unique interface properties of 44BPy in aqueous solution and on the surface of Au(111) electrode (see below). In previous studies, Zhou et al. reported two values for the 44BPy molecular junction conductance, $4.7 \times 10^{-3}G_0$ and 0.59×10^{-3} G_0.[15] Recently, Wang et al. reported a multiple series of the conductance values for Au|44BPy|Au, i.e., $(1.34\pm0.17) \times 10^{-4}$ G_0, $(5.38\pm0.64) \times 10^{-4}$ G_0 and $(75.5\pm15.3) \times 10^{-4}$ G_0, which were attributed to the different binding geometries between the pyridyl anchoring groups and the gold electrodes.[14b] It has been also shown by Quek et al. that 44BPy junction can be reversibly switched between two conductance states by changing the binding geometries.[10]

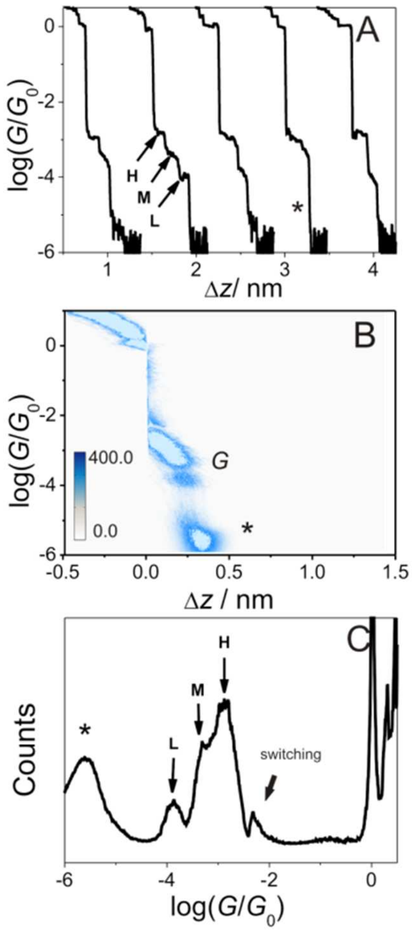

Figure 1. STM-BJ-based conductance measurements of 44BPy in 0.05 M $KClO_4$ containing 0.5 mM 44BPy at applied potential 120 mV vs. Hg/Hg_2SO_4 (MSE) as recorded with V_{bias} = 0.100 V and a stretching rate of 87 nm s^{-1}. (A) Typical original conductance vs. distance traces. (B) 2D conductance histogram generated from 2000 individual curves without any data selection and (C) 1D conductance histogram. The noise level is indicated by the asterix. The small spike at log $(G/G_0) \approx -2.2$ in panel C represents an artefact related to the switching of the amplifier.[16] Hg/Hg_2SO_4 (MSE) and platinum wire were used as reference and counter electrode, respectively.

Figure 2A shows the conductance histograms measured under several electrochemical potentials at pH~5.8 and figure 2B demonstrates the evolution of three conductance features under different electrochemical potentials. The shape of the conductance histogram is quite similar to that we obtained without electrochemical gating except the peak position shifts. The electrochemical potentials were chosen within the entire range of ideally polarized electrode. For detailed information about interfacial phase properties of 44Bpy in electrolyte solution, we refer to work on this topic cited therein.[17] At this pH, 44BPy molecules are assumed to be unprotonated. The potential dependences of all three conductance values are quite similar, which suggests that the level shift due to gating is independent of the binding geometries.

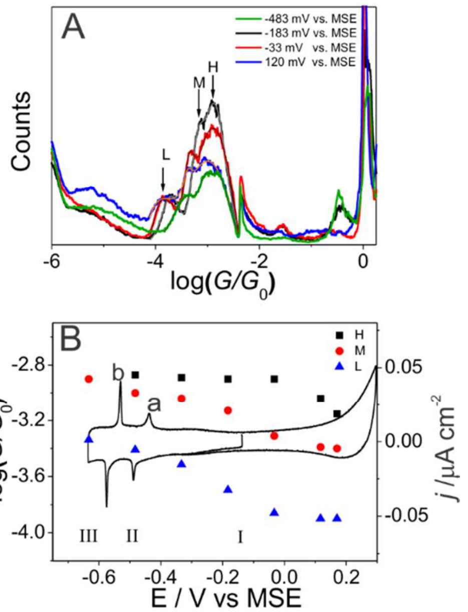

Figure 2. (A) Conductance histograms measured under several electrochemical potentials (B) The most frequently measured conductance as a function of the applied electrode (STM substrate) potential and cyclic voltammogram of the related system at pH 5.8. The experiment was performed in 0.05 M KClO4 as electrolyte containing 0.5mM 44BPy. The bias potential for all the measurements was kept at 100 mV.

According to cyclic voltammogram recorded for 44BPy adsorbed molecules on the surface of Au(111), several regions were defined by the two surface phase transition peaks marked as a and b, which indicated different surface behavior of 44BPy on the Au(111) charged surface. In potential region III of Figure 2B, since the 44BPy molecules are in rhombohedral arrangement with surface coverage of 3.4×10^{-10}mol cm^{-2},[17] the H conductance peaks in the conductance histogram disappear at very negative potentials, because the surface coverage at negative potentials decreases by a factor of 2 and the decreased surface coverage will decrease the probability that two molecules bridge the electrode gap. As mentioned above, the L conductance is associated with elongated junctions containing vertically-aligned molecules attached to electrodes by Au-N bonds and with no π-Au overlap. Therefore the conductance of L is independent of the initial interface configuration of 44BPy on the surface and decreases monotonously with increasing the potential. In region II, the molecular arrangement in the surface is proposed to be a high-order commensurate phase with surface coverage estimated to be 5.7×10^{-10} mol cm^{-2} and the H conductance peak appears, because of the higher probability of trapping two molecules between the leads. Crossing to region I, the molecular arrangement is a close-packed structure with a surface coverage of 6.9×10^{-10}mol cm^{-2} and the conductance decreases compared to the value in region II. In region I, experimental data and theoretical calculations suggest that as the potential sweeps to positive values, the LUMO levels of the molecules move farther away from the electrode Fermi level causing a decrease in conductance. Also, upon increasing to more positive values, the surface charge density on both electrodes increases, and leads to stronger chemical Au-N bonding[18]. A similar trend was also found by Li et. al. who found an increase of ~25% in the conductance of 44BPy by varying the electrochemical potential towards more negative values.[19]

We also studied the effect of varying the pH on the conductance. At pH 10.0, 44BPy showed an enhancement of the conductance, which was almost identical to that obtained by sweeping the potential to negative values (see figure S4A). At pH 4.07, one nitrogen atom of 44BPy is protonated and 44BPy is attached to the surface by the unprotonated terminal pyridine. The repulsive force between the positively charged heads of the molecules prevents the formation of a closely-packed structure on the surface and no clear transition peak between regions I and II was observed (see figure S4B). Although the nitrogen atoms of 44BPy are hydrophilic and can be protonated in acidic solution, the protonation has no effect on the junction conductance, indicating a de-protonation process upon forming the molecule-metal contacts. At pH 1.0, there is no transition peak because at this pH, both of the nitrogen atoms are protonated and the molecules tend to attach to the surface via their π system and block the surface completely (see Figure S4C).

By comparing with theory (see Figure 3), we attribute the enhancement of junction conductance driven by an electrochemical potential to the alignment of the molecular frontier level with the metal Fermi level. Upon sweeping the electrode potential to the negative values, the molecular levels tend to shift downwards and the LUMO level of 44BPy aligns more closely with E_F. Due to the relatively small HOMO-LUMO gap of π-conjugated 44BPy (compared with the "inert" molecules such as saturated alkanedithiols), the level alignment changes from *off*-resonance between molecular frontier level (LUMO) and E_F to "partial" resonance, causing a pronounced increase in the transmission through the 44BPy single-molecule junctions.

Figure 3 shows that for all three sets of conductance groups H, M and L, the increasing trend of the measured conductance with increasing negative gate potential (E_g) aligned well with the tail of LUMO resonance of the transmission coefficient functions. This agreement between the theoretical transmission coefficient curves (evaluated at energy $E-E_F=E_g$) and the observed increasing conductance trend is consistent with the perfectly efficient gating through electrochemical control[5]. (Further details are presented in the SI.) As shown in Figure S6, it is found that the conductance changing rates versus gating voltage for both M and L conductance (10.8×10^{-4} G_0/V and 4.2×10^{-4} G_0/V, respectively) are a factor of 5 higher than the results presented in a recently reported study of the same molecule in organic solvent (1.7×10^{-4} G_0/V and 0.8×10^{-4} G_0/V, respectively, see Figure S6) with ~20% gating efficiency assumed.[4a] This comparison suggested optimal ~100% gating efficiency from the applied potential to the Fermi level shift, which may benefit from the electrochemical highly transparent aqueous electrolyte system used in this work.

We noticed that the present enhancement is different from the "conventional" amplification associated with redox molecules[13]. In the Au|redox|Au system, the modifications of molecular junction conductance are due to electronic structure changes of the redox unit ("inner sphere reorganization energy"), in which redox molecules are usually reduced/oxidized by accepting/removing the electrons. This is not the case for the 44BPy molecules, which keep their neutral state. Therefore, the observed enhancement of the conductance in the present study is expected to be universal for redox-inactive organic molecules with the relative small HOMO-LUMO gap. A more significant gate effect (the stronger resonance) could be expected in the systems with the smaller energetic difference between molecular frontier orbitals and electrode Fermi level or a wider adjustable potential window using other electrolytes instead of aqueous electrolyte.

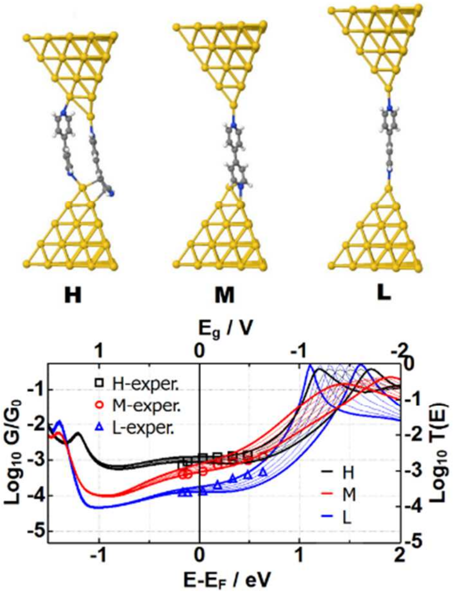

Figure 3. Top: DFT optimized model junction geometries for H, M and L conductance ranges. Bottom: LUMO corrected transmission coefficient functions T(E) for H, M and L model geometries (with bottom and right axes) aligned with the conductance values for various gate potentials (with top and left axes. The data is same as in Figure 2.) LUMO level of the molecule (two molecules for H) is corrected with scissor correction with a range of +1.0…+1.5eV energy shifts. The correspondence between the conductance and the transmission coefficient is $G/G_0=A*T$, where the scaling factor A=0.5 yields the optimal agreement between theory and experiment.

In conclusion, we have studied charge transport through 4,4'-bipyridine (44BPy) single-molecule junctions by employing an STM-based break junction (STM-BJ) technique under electrochemical control and through ab initio simulations based on density functional theory. Qualitative and quantitative agreement between theory and experiment has been demonstrated. We observed three conductance signatures (L, M, and H), which are universal for a variety of environments and electrode potentials. We ascribe the L conductance to the junction configuration in which one 44BPy molecule bonds with the apex gold atoms of the enclosing electrode. The H and M conductances correspond to the junction configuration in which two and one 44BPy molecules bond with the side of highly-coordinated clusters of sites on the electrodes, respectively. More importantly, this work demonstrates that electrochemical gating in aqueous electrolyte provides a viable platform for tuning the charge transport through single-molecule junctions with almost 100% gating efficiency between the electrochemical potential and the alignment of frontier molecular levels.

This work was supported by the Swiss National Science Foundation (Grant No. 200020-144471), EPSRC grants EP/K001507/1, EP/J014753/1, EP/H035818/1 and by EC FP7 ITN

"MOLESCO". We acknowledge particularly the great help from Prof. Dr. Silvio Decurtins on this paper.

Notes and references

[a] Department of Chemistry and Biochemistry, University of Bern, Freiestrasse 3, CH-3012, Bern, Switzerland. Email: hong@dcb.unibe.ch
[b] Department of Physics, Lancaster University, Lancaster LA1 4YB, United Kingdom. Email: c.lambert@lancaster.ac.uk
# These authors contributed equally.

Electronic Supplementary Information (ESI) available: [details of any supplementary information available should be included here]. See DOI: 10.1039/c000000x/

1. A. Aviram and M. A. Ratner, *Chem. Phys. Lett.*, 1974, **29**, 277-283.
2. (a) B. Q. Xu and N. J. J. Tao, *Science*, 2003, **301**, 1221-1223; (b) R. C. Chiechi, E. A. Weiss, M. D. Dickey and G. M. Whitesides, *Angew. Chem. Int. Ed.*, 2008, **47**, 142-144; (c) M. A. Reed, C. Zhou, C. J. Muller, T. P. Burgin and J. M. Tour, *Science*, 1997, **278**, 252-254; (d) E. G. Petrov, A. Marchenko, O. L. Kapitanchuk, N. Katsonis and D. Fichou, *Mol. Cryst. Liq. Cryst.*, 2014, **589**, 3-17.
3. (a) J. Zhang, A. M. Kuznetsov, I. G. Medvedev, Q. Chi, T. Albrecht, P. S. Jensen and J. Ulstrup, *Chem. Rev.*, 2008, **108**, 2737-2791; (b) F. Chen, J. He, C. Nuckolls, T. Roberts, J. E. Klare and S. Lindsay, *Nano Lett.*, 2005, **5**, 503-506; (c) W. Haiss, H. van Zalinge, S. J. Higgins, D. Bethell, H. Hobenreich, D. J. Schiffrin and R. J. Nichols, *J. Am. Chem. Soc.*, 2003, **125**, 15294-15295; (d) I. V. Pobelov, Z. Li and T. Wandlowski, *J. Am. Chem. Soc.*, 2008, **130**, 16045-16054.
4. (a) B. Capozzi, Q. Chen, P. Darancet, M. Kotiuga, M. Buzzeo, J. B. Neaton, C. Nuckolls and L. Venkataraman, *Nano Lett.*, 2014; (b) H. Song, Y. Kim, Y. H. Jang, H. Jeong, M. A. Reed and T. Lee, *Nature*, 2009, **462**, 1039-1043; (c) M. L. Perrin, C. J. O. Verzijl, C. A. Martin, A. J. Shaikh, R. Eelkema, J. H. van Esch, J. M. van Ruitenbeek, J. M. Thijssen, H. S. J. van der Zant and D. Dulic, *Nat. Nanotechnol.*, 2013, **8**, 282-287.
5. S. Trasatti, *Pure Appl. Chem.*, 1986, **58**, 955-966.
6. (a) Z. Li, Y. Liu, S. F. L. Mertens, I. V. Pobelov and T. Wandlowski, *J. Am. Chem. Soc.*, 2010, **132**, 8187-8193; (b) X. Xiao, D. Brune, J. He, S. Lindsay, C. B. Gorman and N. Tao, *Chem. Phys.*, 2006, **326**, 138-143; (c) X.-S. Zhou, L. Liu, P. Fortgang, A.-S. Lefevre, A. Serra-Muns, N. Raouafi, C. Amatore, B.-W. Mao, E. Maisonhaute and B. Schoellhorn, *J. Am. Chem. Soc.*, 2011, **133**, 7509-7516.
7. (a) T. Albrecht, A. Guckian, J. Ulstrup and J. G. Vos, *Nano Lett.*, 2005, **5**, 1451-1455; (b) A. M. Ricci, E. J. Calvo, S. Martin and R. J. Nichols, *J. Am. Chem. Soc.*, 2010, **132**, 2494-+.
8. (a) A. Alessandrini, M. Salerno, S. Frabboni and P. Facci, *Applied Physics Letters*, 2005, **86**; (b) E. A. Della Pia, Q. Chi, D. D. Jones, J. E. Macdonald, J. Ulstrup and M. Elliott, *Nano Lett.*, 2011, **11**, 176-182.
9. (a) P. Petrangolini, A. Alessandrini, L. Berti and P. Facci, *J. Am. Chem. Soc.*, 2010, **132**, 7445-7453; (b) S. Tsoi, I. Griva, S. A. Trammell, A. S. Blum, J. M. Schnur and N. Lebedev, *ACS Nano*, 2008, **2**, 1289-1295.
10. S. Y. Quek, M. Kamenetska, M. L. Steigerwald, H. J. Choi, S. G. Louie, M. S. Hybertsen, J. B. Neaton and L. Venkataraman, *Nat. Nanotechnol.*, 2009, **4**, 230-234.
11. T. Kim, P. Darancet, J. R. Widawsky, M. Kotiuga, S. Y. Quek, J. B. Neaton and L. Venkataraman, *Nano Lett.*, 2014, **14**, 794-798.
12. D. Mayer, T. Dretschkow, K. Ataka and T. Wandlowski, *J. Electroanal. Chem.*, 2002, **524**, 20-35.
13. C. Li, A. Mishchenko, Z. Li, I. Pobelov, W. Th, X. Q. Li, F. Würthner, A. Bagrets and F. Evers, *J. Phys.: Condens. Matter*, 2008, **20**, 374122.
14. (a) M. Kamenetska, S. Y. Quek, A. C. Whalley, M. L. Steigerwald, H. J. Choi, S. G. Louie, C. Nuckolls, M. S. Hybertsen, J. B. Neaton and L. Venkataraman, *J. Am. Chem. Soc.*, 2010, **132**, 6817-6821; (b) C. Wang, A. S. Batsanov, M. R. Bryce, S. Martin, R. J. Nichols, S. J. Higgins, V. M. Garcia-Suarez and C. J. Lambert, *J. Am. Chem. Soc.*, 2009, **131**, 15647-15654.
15. X.-S. Zhou, Z.-B. Chen, S.-H. Liu, S. Jin, L. Liu, H.-M. Zhang, Z.-X. Xie, Y.-B. Jiang and B.-W. Mao, *J. Phys. Chem. C*, 2008, **112**, 3935-3940.
16. W. Hong, D. Z. Manrique, P. Moreno-Garcia, M. Gulcur, A. Mishchenko, C. J. Lambert, M. R. Bryce and T. Wandlowski, *J. Am. Chem. Soc.*, 2012, **134**, 2292-2304.
17. T. Wandlowski, K. Ataka and D. Mayer, *Langmuir*, 2002, **18**, 4331-4341.
18. Z. Liu, S.-Y. Ding, Z.-B. Chen, X. Wang, J.-H. Tian, J. R. Anema, X.-S. Zhou, D.-Y. Wu, B.-W. Mao, X. Xu, B. Ren and Z.-Q. Tian, *Nat. Commun.*, 2011, **2**.
19. X. L. Li, B. Q. Xu, X. Y. Xiao, X. M. Yang, L. Zang and N. J. Tao, *Faraday Discuss.*, 2006, **131**, 111-120.